Submarine pyroclastic deposits formed during the 20th May 2006 dome collapse of the Soufrière Hills volcano, Montserrat

J. Trofimovs[1*], C. Foster[2], R.S.J. Sparks[2], S. Loughlin[3], A. Le Friant[4], C. Deplus[4], L. Porritt[1], T. Christopher[5], R. Luckett[3], P.J., Talling[1], M.R. Palmer[1], T. Le Bas[1]

[1] National Oceanography Centre, Southampton, UK

[2] Department of Earth Sciences, University of Bristol, UK

[3] British Geological Survey, Murchison House, Edinburgh, UK

[4] Institut de Physique du Globe de Paris & CNRS, 4 Place Jussieu, Paris Cedex 05, France

[5] Montserrat Volcano Observatory, Flemings, Montserrat

* Corresponding author: J.Trofimovs@noc.soton.ac.uk,

Address: National Oceanography Centre, European Way, Southampton, UK, SO14 3ZH.

Tel: +44 (0)2380 599239, Fax: +44 (0)2380 596554

Abstract

The 20th May 2006 lava dome collapse of the Soufrière Hills volcano, Montserrat, deposited approximately 115 x 10^6 m^3 non-dense rock equivalent (non-DRE) of material into the ocean. The collapse was rapid with 86% of the mobilized material being removed in just 35 minutes, with a peak volume flux of 66 x 10^3 m^3s^{-1}. Channel and levee facies on the submarine flanks of the volcano and formation of a thick, steep-sided pyroclastic lobe, suggest that the largest and most dense blocks were transported proximally as a high sediment concentration granular flow. Of the submerged volume, 30% was deposited from the base of this granular flow, forming a linear, high relief pyroclastic ridge that extends 7 km from shore. The remaining 70% of the submerged volume comprises the finer grain sizes, which were transported at least 40 km by turbidity currents on gradients of <2°. At several localities the May 2006 distal turbidity currents were observed to have run up 200 m of topography and eroded up to 20 cm of underlying substrate. Multiple depositional subunits are preserved, representing flow reflection from the basin margins and deflection around topography. The high energy of the May 2006 submarine flows resulted in material being transported further than the larger 210 x 10^6 m^3 Soufrière Hills volcano dome collapse in July 2003.

Keywords: Montserrat, dome collapse, pyroclastic flow, submarine, bathymetry

Introduction

The ongoing eruption of the Soufrière Hills volcano, Montserrat, West Indies (Fig. 1) provides an unprecedented opportunity to understand the hazardous, often catastrophic, events that transport sediment into marine environments surrounding island volcanoes. Unusually detailed information is available for both the subaerial and submarine deposits from this volcano. The 1995-present eruption has been monitored in detail on land (e.g. Cole et al., 2002; Herd et al., 2006; Voight et al., 2006), and we are developing a comprehensive and complimentary database for the associated submarine deposits (e.g. Deplus et al., 2001; Le Friant et al., 2004; 2009; Trofimovs et al., 2006; 2008).

This contribution starts by summarising the real-time subaerial observations from a lava dome collapse on the 20th of May 2006 from the Soufrière Hills volcano. Pre- and post-collapse sea floor bathymetry surveys and sediment core data are then used to reconstruct the transport and emplacement processes involved after the pyroclastic flows entered the ocean.

Comparison is made with the submarine deposits from the July 2003 Soufrière Hills volcano dome collapse (Trofimovs et al., 2006; 2008; Le Friant et al., 2009), which was the last major dome collapse from this volcano prior to May 2006. The July 2003 Soufrière Hills volcano dome collapse removed 210 x 10^6 m^3 of the lava dome and deposited 190 x 10^6 m^3 of this into the ocean over a period of ~18 hours. The failure involved four stages (Edmonds and Herd, 2005; Herd et al., 2006): 1) initial low volume pyroclastic flow activity that undermined the central dome complex; 2) three hours of increased pyroclastic flow activity, producing large discrete pyroclastic flows into the ocean; 3) peak collapse conditions involving two hours and forty minutes of semi-continuous pyroclastic flow activity that removed ~170 × 10^6 m^3 from the core of the dome with an average flux of 1 × 10^6 m^3/minute; and 4) small volume, slope stabilising pyroclastic flows that occurred for several hours after the main collapse.

The submarine deposits resulting from the July 2003 dome collapse comprise two linear, steep-sided proximal pyroclastic ridges extending 7 km from the shore (Trofimovs et al., 2006; Le Friant et al., 2009). Propagating from these proximal lobes was a single turbidite deposit that spread across the Bouillante-Montserrat graben (Fig. 1) (Trofimovs et al., 2008). The July 2003 dome collapse of the Soufrière Hills volcano provided the opportunity to reconstruct the real time subaerial collapse chronology, volume flux into the ocean, and the resulting submarine deposits. A second well-documented dome collapse into the ocean occurred on the 20th May 2006 (Loughlin et al., 2006; Luckett et al., 2008; Loughlin et al., 2010), and the characterisation of these submarine deposits is the principal topic of this paper. The May 2006 collapse was much shorter in duration but more intense than in July 2003 (Loughlin et al., 2006). This difference allows us to investigate how source conditions of the flow into the ocean affect the resulting submarine deposits.

Geological Background

The island of Montserrat lies at 16°45' N, 62°10' W, within the northern section of the Lesser Antilles Arc in the Caribbean Sea (Fig. 1 inset). The volcanic arc is the result of the North American plate being subducted beneath the Caribbean plate at a convergence rate of 2-4 cm/year (Bouysse et al., 1990; Grindlay et al., 2005). The island is 16 km long and 10 km wide and comprises three volcanic massifs. To the north of the island the Silver Hills (2600 – 1200 ka) and Centre Hills (950 – 550 ka) are extinct and have been subject to significant erosion (Harford et al., 2002). The South Soufrière Hills-Soufrière Hills massif shows evidence of volcanic activity going back at least 170 ka (Harford et al., 2002), and is the location of the current eruption.

The current eruption of the Soufrière Hills Volcano on Montserrat, which began in 1995, is the most destructive event in the Lesser Antilles volcanic arc since the eruption of Mont Pelée on the island of Martinique in 1902 (Kokelaar, 2002). The Soufrière Hills volcanic massif had been volcanically inactive for an estimated 350 years when, on the 18th of July 1995, phreatic explosions began on the flank of a dormant lava dome situated within English's Crater, a four thousand year old collapse scar. The extrusion of a new andesitic dome started some 18 weeks later. Over the next 60 weeks, lava dome collapse, pyroclastic flow activity and one episode of violent explosivity filled in the old crater.

Devastation was brought to the island in 1997. Major dome collapses generated pyroclastic flows, which left thick deposits over the main port and capital city of Plymouth. The island's airport was inundated with ash and tephra fall out, and homes, vegetation and livelihoods were destroyed over large parts of the island. Nineteen people were killed and several injured on June 25 1997 as a direct result of the volcanic activity (Loughlin et al., 2002).

Since it began, the current eruption has been characterized by protracted periods of andesite lava dome growth and collapse, forming block-and-ash pyroclastic flows. The proximity of the volcano to the ocean has led to >75% of the eruptive products being distributed into the sea (Le Friant et al., 2009).

On the 12-13th July 2003 the largest lava dome collapse in recorded history occurred, producing ~210 million cubic metres of material, which avalanched down the Tar River Valley (Fig. 1) to the east of the island (Herd et al., 2006). Pyroclastic flows large enough to reach the sea caused additional hazards; pyroclastic surge clouds traveled up to 3 km across the ocean surface before dissipating; phreatic explosions, the result of instantaneous boiling of sea water when the hot pyroclastic debris reached the ocean, drove hot ash clouds back inland, burning vegetation and depositing thick layers of fine material; and the impact of millions of cubic metres of material avalanching into the ocean generated tsunamis that caused damage on neighbouring islands (Edmonds and Herd, 2005; Herd et al., 2006).

On the 20th of May 2006 another major dome collapse occurred, resulting in large amounts of pyroclastic material being transported into the sea via the Tar River Valley off the eastern Montserrat coast (Loughlin et al., 2006). This collapse resulted in significant new deposits being laid down off the east coast of the island.

Methods

This study uses a multi-disciplinary approach to analyse real-time subaerial observations of the May 2006 dome collapse, together with submarine geophysical surveys and core samples collected during the JC18 research cruise on the RRS *James Cook* (3-16 December 2007), with pre-event bathymetry collected during the JR123 research cruise of the RRS *James Clark Ross* (9-18 May 2005). Figure 1 shows the area covered by the JC18 cruise, the bathymetry and core locations.

JC18 Bathymetry

A high-resolution EM120 swath bathymetry survey was recovered off the east coast of Montserrat. The survey equipment generated 191 across track beams within an angle of 150°. The ship was traveling at an average 2 m s^{-1}, and water depths ranged from 300 to 1200 m. Sea conditions for the cruise were favourable and thus a single velocity profile was used for conversion from travel times to depth. No tidal corrections were used, as the tidal movement was less than 0.5 m. Depth errors had a median standard deviation of 2.3 m, which is approximately 0.25% of total depth and is very good for the system. The maximum lateral errors are 10 m along track and 47 m across track; maximum depth error is 7 m. The data quality was very high and thus allowed gridding at 50 m.

Previous Bathymetric Survey Data

The bathymetry of the study region has been surveyed five times since the current eruption began: Seapony (July 1998), Aguadomar (Dec 1998 – Jan 1999), Caraval (Feb 2002), JR123 (May 2005) and JC18 (Dec 2007). The results of the first four surveys have been reported in Deplus et al. (2001), Hart et al. (2004), Trofimovs et al. (2006; 2008) and Le Friant et al. (2009). The fifth survey provides new data and is part of this contribution. A British naval survey by HMS Fawn in 1985 provides the pre-eruption bathymetry.

HMS Fawn surveyed an area that included the region offshore from the Tar River Valley (Fig. 1), and provides the benchmark bathymetry that has subsequently been modified by erosion and deposition associated with submarine pyroclastic flow activity. The second survey considered in this study (JR123) identified submarine deposits formed between the start of the eruption (1995) and 2005, and by comparison with earlier surveys identified the deposits formed by the dome collapse of July 2003 (Trofimovs et al., 2006; 2008). The third survey considered herein (JC18) collected data on the deposits that resulted from the major dome collapse on the 20th May 2006.

Comparing pre- and post-May 2006 collapse sea floor bathymetric surveys produced images of the submarine deposits resulting from the May 2006 dome collapse. Estimates for the May 20th 2006 deposits were generated from a comparison of gridded data from the JC18 (2007) survey with the survey of the same area from the JR123 research cruise of 2005 (Trofimovs et al., 2006; 2008). The two surveys used similar onboard EM120 swath bathymetry systems and dynamic ship positioning, therefore the two data sets are comparable.

Seafloor Sampling

The submarine deposits from the May 2006 dome collapse were sampled *in situ* using gravity core and megacore rigs; 35 cores were recovered in total. The gravity cores recovered up to 2.5 m of unconsolidated sediment. This system was not well suited to the coarse grained nature of the most proximal pyroclastic deposits and consequently samples were only recovered within the finer grained, medial to distal reaches of the May 2006 dome collapse deposits. Occasionally the gravity coring resulted in the loss of the fine grained, upper few centimeters of sediment. Megacores in these positions, however, recovered shorter (<80 cm) core samples, but with good preservation of the uppermost sedimentary layers and the sediment-water interface.

The recovered cores were split on board and stratigraphically logged at appropriate scales. They were then put in cold storage at 4-5°C before sub-sampling on land. Samples of ~1 cm^3 were taken for component and grain size analysis. Component abundance was determined by point counting a minimum of 500 grains for each targeted sample. Grain size analysis used a Malvern laser particle size analyser (Mastersizer 2000). The Malvern can measure particles up to 2 mm in diameter, therefore the samples were passed through a 2 mm sieve before Malvern analysis.

Only two of the 227 samples measured contained clasts larger than 2 mm. These large particles (only four in total) were isolated and measured separately by hand.

The samples for Malvern analysis was mixed with 50 ml of deionised water with 0.05% Calgon (a polyphosphate dispersion reagent) and left on a shaking table overnight (~12 hr). The Malvern passes a narrow beam of monochromatic light through the sample wherein the particles diffract the light at a given angle. That angle increases with decreasing particle size. The particles were kept in suspension using in-built stirrers and the sample was pumped continuously through the Malvern to ensure random orientation of the particles relative to the laser beam. Pump and stirrer speeds were constant throughout all analyses. Light obscuration was between 10 and 20%. Three measurements were taken for all samples for quality control.

The May 2006 dome collapse deposits were identified proximally without ambiguity, using seafloor bathymetry maps. Further from shore the May 2006 deposits were assumed to represent the last major episode of sedimentation (the uppermost unit). Where available, the stratigraphy from cores in similar locations, recovered before and after the May 2006 collapse (from the JR123 and JC18 cruises respectively), were compared. This allowed unambiguous identification of the newly emplaced May 2006 dome collapse deposits.

Subaerial Collapse Chronology for the 20 May 2006 dome collapse

The following chronology is taken from Loughlin et al. (2006), Luckett et al. (2008) and Loughlin et al. (2010). The dome collapse on the 20th May 2006 involved the removal of approximately 115 x 10^6 m^3 of rock over a period of less than 3 hours; approximately 86% of the dome collapsed in just 35 minutes. Dome collapse activity started just after 6 am (local time) on 20th May 2006. A large long period earthquake immediately preceded the dome collapse, which was also accompanied by heavy rain and an increase in dome growth rate during the week preceding the eruption. The dome collapse progressed through 3 stages. The first stage lasted ~1.5 hrs (between 06:11 and 07:32) during which rockfalls and pyroclastic flows removed material almost continuously from the margins of the dome. The second stage, beginning at 07:32, was 35 minutes in duration and involved the bulk of the collapse. During this stage, at 07:36, a pyroclastic flow with two main peaks in flux was observed entering the sea off the Tar River Valley. As the bulk of the flow was submerged a dilute surge cloud decoupled from the flow and traveled ~3 km over the ocean surface before losing momentum and settling into the water. At 07:43, another pulse generated a vertical steam and ash plume approximately 17 km high. Concurrently hydrovolcanic explosions at the coastline generated pyroclastic density currents that traveled rapidly northwards along the coast for 3 km, and 500 m back inland towards the volcano reaching a height of 168 m above sea level. No pyroclastic density currents were observed towards the south. Associated with peak collapse conditions (Stage 2), a 1 m high tsunami was recorded in the Deshais Harbour and Les Saints in Guadeloupe, and swells of 30 cm were recorded on the southeast coast of Antigua and west coast of Montserrat. Intense pyroclastic flow activity ceased at 8.07 am, signaling the end of Stage 2. The level of activity dramatically declined in the third stage. Two discrete pyroclastic flows were observed reaching the sea at 08:25 and 08:35, but activity was almost at background levels by 09:00. Heavy rain and ash fall combined to cause highly erosive lahars in all drainage channels on the volcano including the Tar River Valley just before and during the early part of Stage 1 of the collapse.

Passage of pyroclastic flows carved a channel approximately 500 m wide through the pre-existing Tar River Valley delta (Fig. 2). The channel was partially infilled with pyroclastic flow deposits during the waning Stage 3. The pyroclastic density currents associated with littoral explosions deposited up to 0.5 m of ash on the delta and eastern flanks of the volcano, north of the flow channel and as far as Spanish Point (Fig. 1).

The volume of the lava dome calculated on 18 May 2006 using ground-based LiDAR was 101 x 10^6 m^3 non-DRE (Jones, 2006) and 85.2 x 10^6 m^3 dense rock equivalent (DRE) (Ryan et al., 2010). The total collapse volume, including eroded and incorporated older dome remnants and crater wall material, was estimated at about 115 x 10^6 m^3 non-DRE and 97 x 10^6 m^3 DRE with an error of about ±15% using estimated extrusion rates and photogrammetric assessments (Ryan et al., 2010; Loughlin et al., 2010). Montserrat Volcano Observatory staff used Real-time Seismic Amplitude Measurements (RSAM; Endo and Murray, 1992; Brodscholl et al., 2000) and seismic velocity to assess the volume of collapsed material as a function of time (*BGS unpublished data*). This method has been successfully applied to previous Montserrat collapses in 2000 (Carn et al., 2004) and 2003 (Herd et al., 2006). Analysis of the total volume of material removed as a function of time suggests an estimated 9% was removed during Stage 1 (6:00 to 7:32 am), 47% during the first peak phase of Stage 2 (7:32- 7:45 am), 39% during the second peak phase of Stage 2 (7:45-8:07am) and 4% during Stage 3 (8:07 – 09:00am). Therefore, non-DRE volume estimates for each stage of the collapse are: Stage 1, 10.35 x 10^6 m^3; Stage 2A, 54.05 x 10^6 m^3; Stage 2B, 44.85 x 10^6 m^3; and Stage 3, 4.6 x 10^6 m^3.

Submarine pyroclastic deposits from the May 2006 dome collapse

Sea floor morphology at the base of the Tar River Valley

A large embayment in the submarine flanks of the volcano is visible in the JR123 and JC18 bathymetric images (Fig. 3a and 3b), with infilling hummocky terrain that fans out towards the east. The embayment is the submarine extension of the subaerial English's Crater (Le Friant et al., 2004), within which the current eruption is venting. English's Crater was formed by two large volume landslides at 3950 +/- 70 and 1940 +/- 35 years ago (Roobol and Smith, 1998; Boudon et al., 2007). The hummocky sediment infill within the submarine embayment largely represents the debris avalanche deposits from these two landslides (Le Friant et al., 2004) together with pyroclastic deposits from the current Soufrière Hills volcano eruption (e.g. Hart et al., 2004; Trofimovs et al., 2008; Le Friant et al., 2009).

Analysis of the 2005 bathymetric survey (JR123; Fig. 3a) shows a prominent east-west trending ridge (marked as R) within the submarine embayment around latitude 16.72° N. This ridge extends approximately 7 km offshore and is best-developed 4 to 7 km from shore. Trofimovs et al. (2006) and Le Friant et al. (2009) report that this ridge is predominantly the product of the July 2003 dome collapse from the Soufrière Hills volcano. This feature has been partially obscured in the latter 2007 bathymetric survey. The current seafloor morphology exhibits a new near-linear, east west trending ridge at latitude 16.72° N (Fig. 3b). Close to the shore (longitude 62.135° W to 62.12° W) the ridge has a central depression bounded by two topographic highs (marked D in Fig. 3b).

May 2006 dome collapse proximal submarine deposit morphology

Comparison of the May 2005 (JR123) and December 2007 (JC18) bathymetric surveys produces a topographic difference map (Fig. 4a and 4b) that highlights the deposits emplaced during the 20th May 2006 dome collapse; the only major volcanic event down the Tar River Valley recorded between these dates. The morphology of the May 2006 deposits are such that the deposits form a linear feature following a single trajectory to create a narrow east-west structure slightly to the north of the thickest pre-2005 deposits.

The May 2006 dome collapse deposits can be divided into distinct morphological regions. Near shore, the deposit shows two linear topographic highs either side of a linear depression within which the sea floor depth has changed little since the previous 2005 survey. Further offshore, just beyond the linear depression, the deposits form a positive relief linear ridge with a maximum thickness of ~54 m. The ridge thins down slope, away from source.

Cross sectional profiles of the 1985, 2005 and 2007 bathymetry surveys show how the current eruption of the Soufrière Hills volcano has altered the sea floor. An east-west trending profile down the axis of the May 2006 deposits (Fig. 5) illustrates how the submarine pyroclastic fan has developed. The 2005 surface (shown in green) shows a tapering, yet evenly distributed, thickness of deposited pyroclastic material independent of the steep sea floor gradient in the proximal regions, and shallower distal slopes. Deposition occurred on slopes of at least 11°. The deposit thickness difference between the 1985 pre-eruption bathymetry (red line) and the green 2005 survey line represents an amalgamation of deposits emplaced between these two dates (Deplus et al., 2001; Hart et al., 2004; Trofimovs et al., 2006; 2008; Le Friant et al., 2009). We use the 2005 survey data herein to clearly define the base of the May 2006 deposits.

The May 2006 dome collapse deposit (shown in blue) is restricted to slopes of less than or equal to 7°. The deposit reaches a maximum thickness of 54 m four kilometres from shore, in a region of marked slope change (from ~11° to <7°). Further down slope the deposits thin to form a tapering wedge. The limit of geophysical resolution for the May 2006 deposits ends approximately 7 km from shore. Therefore, the length of the imaged constructional feature is ~3.5 km.

North-south cross-sectional profiles (Fig. 6), approximately parallel to the shoreline and normal to the flow direction, show the distribution of pyroclastic material with distance from source. All profiles show the pre-eruption surface in red, the 2005 surface in green and the 2007 surface in blue, and have a vertical exaggeration of x6.

In the proximal parts of the fan (e.g. Fig. 6b), the majority of the deposits formed within the boundaries of the submarine extension of English's Crater. The May 2006 deposits, at this point, consist largely of two topographic ridges bordering a distinct linear topographic low. The linear indentation is over 2 km in length, and runs parallel to the inferred direction of flow (Fig. 4). At some points the axis of the indentation lies below the pre-existing (2005) sea floor (Fig. 4 and 6b).

Approximately 3 km from the coast the southern margin of the submarine extension of English's Crater decreases from 75 m to 50 m above the internal crater floor, at which point the current eruption products overtop the scarp (Fig. 6c). At this point, which also corresponds to a break in slope, the May 2006 deposits are thickest. The deposits thin with distance from the shore (Fig. 6d) until they taper out approximately 7 km from the coast.

Volume of the May 2006 proximal submarine deposits

A volume of 40 x 10^6 m^3 non-DRE has been calculated for the proximal linear ridge formed by the May 2006 dome collapse into the ocean. The volume calculation for this proximal deposit is based on the 2005-2007 topographic difference map, where all measurements greater than 5 m thickness are included. This technique is comparable to that used by Le Friant et al. (2009), who reported on the distribution of volcanic material from the 1995-2005 events from the Soufrière Hills volcano. The average depth error for JC18 data is ±2 m; therefore these calculations provide a minimum volume.

May 2006 dome collapse medial to distal submarine deposits

The thinner medial to distal reaches of the May 2006 submarine pyroclastic deposits were beyond the resolution of the bathymetry survey and are only documented by coring. Figure 7 shows the location of the recovered cores and the thickness of the preserved May 2006 deposits. Coring was focused within the Bouillante-Montserrat graben, a fault-bounded basin southeast of Montserrat (Fig. 1), within which the majority of the Tar River Valley pyroclastic flow deposits are located. The proximal deposits imaged by the bathymetry were too coarse grained to core successfully with available equipment. Therefore only the finer grained, more distal deposits were sampled. Stratigraphic logs taken along the axis of the May 2006 deposit show that it comprises a complex series of subunits that cannot be correlated between cores, some of which are only hundreds of metres apart (Fig. 8). The May 2006 flows were predominantly confined within the Bouillante-Montserrat graben, as the thickest, coarsest grained deposits are found within the basin axis, with deposits becoming thinner and finer grained towards the margins (Fig. 8 and 9). The centre of the graben contains fewer subunits than the basin margins, where multiple finer grained deposits are commonly preserved (Fig. 9).

At the most proximal cored location within the main flow axis, JC18-07-M (Fig. 10), a short (26 cm) core intersects two volcaniclastic subunits; the uppermost subunit has an erosive, inversely graded base, whereas the base of the lower subunit was not intersected. Both subunits preserve a normally graded top, range from poorly to moderately well sorted (1.54-0.68 σ_ϕ), and show predominantly sand sized particles (1.75-2.5 M_ϕ) at the base of the subunits and fine sand to silt sized particles (>3.0 M_ϕ) at their tops. Crude planar laminations are observed in the uppermost subunit. The components comprise juvenile andesitic lava dome fragments (70%), hydrothermally altered andesite fragments (15%), angular, broken hornblende, plagioclase and subordinate pyroxene crystals (14%), and 1% bioclastic material eroded and incorporated from the substrate.

Cores recovered along the main flow axis preserve between one and six depositional subunits (Fig. 8). Little variation in components and component abundances, a lack of consistent sedimentary structures and significant differences in subunit thickness make it difficult to correlate subunits between cores. For example, cores JC18-08-B and JC18-33-B are located just 560 m from each other, yet they exhibit significantly different stratigraphy. Six subunits were emplaced during the May 2006 dome collapse, as recognized in JC18-08-B. These overlie two pre-existing depositional units from earlier Soufrière Hills collapses that were identified in previous core sites collected during the JR123 cruise in May 2005. JC18-33-B only preserved two subunits that are significantly thicker than their counterparts in JC18-08-B. However, the basal subunit in JC18-33-B shows an erosive bottom contact, therefore implying that other subunits may have been eroded away.

The single, 50 cm thick, deposit observed in JC18-10-M (Fig. 11) shows that the mass flows resulting from the May 2006 collapse were significantly erosive. This core was taken adjacent to a core site (JR123-8-V) from the JR123 cruise. The pre-May 2006 stratigraphy showed two volcaniclastic turbidites, with a total thickness of 16 cm. These deposits were the result of the July 2003, and possibly the July 2001, dome collapses from the Soufrière Hills volcano (Trofimovs et al., 2006; 2008). Subsequent to the May 2006 dome collapse, only a single depositional unit of 50 cm was present at this site. This implies that the previous volcaniclastic deposits and possibly underlying hemipelagic sediment was eroded by and incorporated into the May 2006 volcaniclastic flow.

At the most distal cored extent (JC18-12-M; Fig. 12), approximately 43 km from the Montserrat coast, a stacked series of four fine-grained, centimeter-scale volcaniclastic depositional units are preserved. At this location no cores had previously been collected. Therefore, without a previous stratigraphic sequence for comparison, we could not unambiguously determine whether the lower-most subunit in core JC18-12-

M is the deposit of the May 2006 dome collapse or the previous July 2003 dome collapse of the Soufrière Hills volcano (Trofimovs et al., 2008). We include grain size analysis for all four subunits. The subunits are all normally graded and exhibit erosive scours at their bases. They are characterised by poorly sorted (1.12-1.68 σ_{ϕ}), fine sand, silt and clay sized particles (2.0 ϕ to <10 ϕ; median diameters <4 ϕ). Millimetre-scale planar laminations are observed centrally within the thickest subunit. Stratification is defined by bioclast-rich (~5% bioclasts) and bioclast–poor (<1% bioclasts) laminae.

Stratigraphic transects perpendicular to the main flow axis show the flow deposits thin and fine towards the basin margins (Fig. 9). The western edge of the Bouillante-Montserrat graben shows a stacked series of centimeter-scale fine sand and silt depositional units. Erosive bases are common, as are millimeter-scale planar laminations and rare cross-lamination. Core JC18-32-M is situated within a saddle between two seamounts on the eastern margin of the basin. This core site lies ~200 m above the basin floor up steep topography, yet two depositional units attributed to the May 2006 dome collapse are observed.

Volume of the May 2006 medial to distal submarine deposits

An isopach map based on the cored thickness of the May 2006 dome collapse deposits shows ~90 x 10^6 m^3 of sediment was deposited downstream from the proximal pyroclastic ridge (Fig. 7). This is a minimum estimate as the most distal reaches of the deposits were not intersected and it is expected that a percentage of the finest grain sizes were removed from the study region by the lofting of ash (c.f. Cole et al., 2002) and ocean currents.

Therefore, the submarine deposits for the May 2006 dome collapse total ~130 x 10^6 m^3 (90 x 10^6 m^3 medial to distal and 40 x 10^6 m^3 proximal). This equates to ~109 × 10^6 m^3 dense rock equivalent (DRE), using a measured average clast density of 1900 kg/m^3 and average submarine sediment density as 1600 kg/m^3 (measured when dried).

Discussion and Interpretations

Seafloor Morphological Features

In the proximal part of the pre-eruption fan, successive dome collapse deposits have filled in a depression, which we identify as the submarine extension of the Tar River Valley. This depression lies within the deep channel described by Deplus et al. (2001) and identified as part of the scar caused by the two flank collapses that created English's Crater approximately 3950 and 1940 years ago (Roobol and Smith, 1998; Boudon et al., 2007). The submarine pyroclastic deposits do not extend laterally beyond the constraining scarps of the depression, but form a constructive ridge on slopes up to 11° (Fig. 6).

Depositional processes: proximal May 2006 deposits

The most proximal of the submarine May 2006 deposits consists of two parallel ridges separated by a topographic low. This feature is interpreted as showing a channel-levée morphology. In places the channel cuts down into the pre-May 2006 seascape, evidencing erosion of previously deposited material (Fig. 4). In other areas the central channel appears only to be a region of non-deposition. The submarine channel lies directly downstream from the erosive channel on the subaerial pyroclastic fan at the base of the Tar River Valley. The length of the submarine channel is more than 3 km.

The formation of a well-defined straight-sided channel with steep sided bounding levées, combined with no evidence for deposition outside the levées, places constraints on the nature of the depositing flow. This morphology is characteristic of high sediment concentration granular flows (e.g. Nairn and Self, 1978; Ui et al., 1999; Calder et al., 2000). The levées reflect the height of the flow at peak flux (Felix and Thomas, 2004). The central depression represents where the flow has drained from the channel in the later stages of emplacement (Felix and Thomas, 2004), in this case to be deposited down slope as the high relief pyroclastic ridge. Similar channel-levee morphologies have been observed associated with small volume pyroclastic density currents resulting from either dome or column collapse in the subaerial environment (e.g. Rodriguez-Elizarraras et al., 1991; Saucedo et al., 2004; Lube et al., 2007). Earlier small volume dome collapses from the current Soufrière Hills volcano eruption have produced steep-sided lobate deposits with well-developed levees (Cole et al., 2002). Lube et al. (2007) document subaerial channel and levée deposits from the 1975 Ngauruhoe eruption, New Zealand. Small volume, low energy, dense pyroclastic granular flows produced coarse grained, fines-poor levées around a channel partially infilled with ash-rich, clast- to matrix-supported breccia on slopes < 25°. We assume similar emplacement mechanisms for the submarine deposits to those observed on land.

Downstream from the channel-levee facies, deposited at a break in slope from ~11° to 7°, is the 3.5 km long pyroclastic ridge. The ridge is ~1 km wide at its widest point and tapers towards its distal reaches. The lack of lateral spreading on the unconfined shallow slopes provides further evidence that these were formed by high concentration granular flows. As we were unable to core the proximal May 2006 pyroclastic ridge we can only hypothesise as to the nature of the deposit. However, coring of the analogous proximal submarine deposits from the July 2003 dome collapse from the Soufrière Hills volcano (Trofimovs et al., 2008) suggested that as the pyroclastic flows entered the ocean they rapidly mixed with seawater and that the finer grained material was efficiently elutriated into the overlying water column. The large dense blocks were deposited proximally, generally at breaks in slope, from the dense granular flows. Further cores taken adjacent to the lateral margins of the proximal July 2003 deposits showed undisturbed pre-eruption hemipelagic sediment, indicating that the pyroclastic ridge margins were quite sharp (Trofimovs et al., 2006; 2008).

Depositional processes: medial to distal May 2006 deposits

The cored medial to distal reaches of the May 2006 deposits preserve multiple depositional units. The bases of the subunits exhibit evidence of erosion of underlying strata, show the coarsest grain sizes and are commonly massive. The central to upper parts of each subunit show normal grain size grading, often with tractional features such as planar and rare cross laminae. The deposit is more extensive and tabular in morphology than the proximal pyroclastic ridges, although predominantly confined within the Bouillante-Montserrat graben.

The well-developed vertical grading and tractional structures are indicative of deposition from a progressively aggrading turbidity current (e.g. Kuenen, 1966; Allen, 1971; Kneller and Buckee, 2000). The fine grained top and planar to ripple cross-laminae in particular, are typical of Bouma divisions b, c and e (Bouma, 1962). However, the presence of multiple turbidite subunits, together with the variation and distribution of the sedimentary structures within the subunits, is indicative of complex flow history and dynamics.

Origin of multiple subunits

The formation of multiple subunits can be attributed to flow reflection off the basin margins, deflection around seafloor topography, or multiple flow pulses from the original collapse into the ocean. The period of peak collapse conditions, which supplied the bulk of the material deposited into the ocean, had a duration of 35 minutes. During this time there was continuous entrance of pyroclastic material into the ocean, although in the form of two pulses. These two pulses of high flux could account for two separate, relatively large, depositional units, where the fast flow front of the second pulse catches up with, and overtakes, the slower tail of the first pulse (c.f. Kneller and McCaffrey, 2003). Small volume pyroclastic flows in the waning stage (Stage 3) of collapse may have provided additional, somewhat smaller and less extensive depositional subunits.

A likely scenario explaining the formation of some of the turbidite subunits is through flow reflection. Although it is difficult to correlate individual subunits between cores, it is apparent that the number of subunits increases towards the basin margins (Fig. 9). The basin margins also preserve the thinner, finer grained depositional units. Kneller and McCaffrey (1999) describe the finer grained, more dilute upper part of a turbidity current decoupling from the denser basal section, and running up the margins of confining topography. The dilute flow loses momentum and collapses back into the basin forming secondary flows perpendicular to the basin margins. We envisage similar processes occurring with the May 2006 turbidity currents.

Flow deflection (c.f. Kneller and McCaffrey, 1999; Kneller and Buckee, 2000) around pre-existing high relief topography could result in flow separation and the deposition of multiple subunits. Le Friant et al. (2004) imaged megablocks within the Bouillante-Montserrat graben several ten's of metres high. Turbulent flow over and around such objects affects flow velocity and density. Upstream of the obstacle the flow experiences rapid deceleration and sedimentation is likely (Kneller and Buckee, 2000). Downstream from the obstacle the flow, or part thereof, may diverge from its original course or the flow may separate according to density and velocity.

Deposit Volumes

Subaerial measurements estimate 115 x 10^6 m^3 (non-DRE) of pyroclastic material was mobilised during the May 2006 dome collapse. The majority of the material was deposited into the ocean, although a proportion (~4-16%; Bonadonna et al., 2002) of fine ash was lofted into the atmosphere as buoyant plumes. Of the volume that entered the ocean, 40 x 10^6 m^3 remained within the proximal area and 90 x 10^6 m^3 was deposited medially to distally (equating to 130 x 10^6 m^3 of sediment, or 109 x 10^6 m^3 DRE). As the submarine volumes provided are minimum estimates, it is likely that they are under representations. Therefore the submarine deposits represent a larger volume of material than that which originally entered the ocean during the dome collapse. The additional material was likely derived from erosion and incorporation of underlying strata on the flanks of the volcano and within the Bouillante-Montserrat graben. The proximal channel-levee system shows erosion within the channel axis and more distal cores, such as JC18-10-M, exhibit significant erosion at the base of the May 2006 deposit. Bioclastic material within the May 2006 deposits provides evidence for the erosion and incorporation of hemipelagic sediment as well as underlying volcaniclastic deposits.

The proportion of May 2006 sediment deposited within the proximal ridge, compared with that deposited more distally is 30% proximal versus 70% medial to distal. This contrasts with the previous dome collapse on Montserrat in July 2003 (Herd et al., 2006), where the 210 x 10^6 m^3 collapse deposited 69% of its volume proximally and 31% medially to distally (Trofimovs et al., 2008; Le Friant et al., 2009).

Volume flux into the ocean

The July 2003 dome collapse involved a volume of material nearly twice that of the May 2006 dome collapse. However, the July 2003 collapse occurred over an ~18-hour period (Herd et al., 2006), whereas the May 2006 dome collapsed in less than 3 hours, with peak activity focussed into 35 minutes. A comparison of the estimated volume fluxes for the 2003 and 2006 collapses of the Soufrière Hills volcano shows that, apart from 2 minutes of peak activity, the average flux of the July 2003 dome collapse was approximately one third of the May 2006 event (Table 1).

Table 1: Comparison of subaerial volume flux estimates for July 2003 and May 2006 dome collapse events. Volumes are non-DRE.

	July 2003 (from Herd et al., 2006)	May 2006
Entire collapse	210 x 10^6 m^3 in 18 hrs mean flux = 3.2 x 10^3 m^3s^{-1}	115 x 10^6 m^3 in 3 hrs mean flux = 10.6 x 10^3 m^3s^{-1}
Most Intense Stage	170 x 10^6 m^3 (81%) in 2.6 hrs mean flux = 18.2 x 10^3 m^3s^{-1}	98.9 x 10^6 m^3 (86%) in 35 mins mean flux = 47.1 x 10^3 m^3s^{-1}
Peak Conditions	16 x 10^6 m^3 (8%) in 2 mins mean flux = 133 x 10^3 m^3s^{-1}	54.05 x 10^6 m^3 (47%) in 13 mins mean flux = 69.3 x 10^3 m^3s^{-1}

Comparison of the July 2003 and May 2006 submarine pyroclastic deposits

Although smaller in volume, the May 2006 dome collapse had a higher volume flux into the ocean than the July 2003 collapse. The greater flux may account for the fact that the May 2006 flows deposited a greater amount of sediment further from the shore, when compared with the 2003 collapse. The pyroclastic ridges that resulted from the May 2006 and July 2003 collapses both deposited the largest and densest blocks up to 7 km from shore (Trofimovs et al., 2006). Proportionally, 70% of the May 2006 transported volume was deposited downstream from the proximal pyroclastic ridge, compared to 31% in July 2003.

Previous studies of the on-land products of the current Soufrière Hills volcano eruption show that the subaerial pyroclastic flows contain approximately 50% blocks and 50% ash (Cole et al., 2002). Coring the pyroclastic ridge deposited during the

July 2003 dome collapse showed that the majority of the ash was efficiently removed from the proximal deposits and transported distally (Trofimovs et al., 2008). The finer grained, sand to ash-sized particles largely account for the more distal turbidite deposits. The high proportion (70%) of fine-grained distal deposits associated with the May 2006 collapse can likely be attributed to the high energy of the collapse. The high-energy collapse dynamics produced a large abundance of fine material, perhaps a proportionally larger abundance than the lower energy collapses previously observed on Montserrat (Cole et al., 2002; Herd et al., 2006). This fine material was efficiently elutriated into the water column as the pyroclastic flow entered the ocean, where it continued to flow as a more dilute turbidity current.

The high momentum of the submarine flows is additionally indicated by the presence of two May 2006 flow deposits situated ~200 m above the Bouillante-Montserrat graben floor (core site JC18-32-M). The deposits exhibit a sandy base overlain by planar laminae and an ash-rich top. The coarser-grained base and presence of tractional sedimentary structures suggests that the turbidity current ran up the steep topography to the elevated depositional site, as opposed to being a dilute flow inflated to a thickness equivalent to the height of the saddle between the seamounts. There is no evidence of the July 2003 deposits running up similar topography.

The May 2006 turbidity currents transported a greater volume of coarser grained material further than the July 2003 deposit. At the furthest cored extent (JC18-12-G; ~43 km SE from Montserrat) the May 2006 deposits are thicker and coarser grained than the previously emplaced July 2003 deposits. In places there has been complete removal of the pre-existing volcaniclastic deposits by the highly erosive May 2006 flows.

Conclusions

Approximately 115 x 10^6 m^3 non-DRE of pyroclastic material entered the ocean as a result of lava dome collapse at the Soufrière Hills volcano on the 20th of May 2006. The bulk of the material (86%) collapsed within only 35 minutes giving an estimated peak volume flux of 69.3 x 10^3 m^3s^{-1}. Around 30% of the submarine volume was deposited as a narrow linear ridge that extends 7 km from the shoreline. Proximal channel and levee facies are observed implying deposition from a high sediment concentration granular flow. The remaining 70% of the deposited volume was transported downstream for more than 40 km by dilute turbidity currents.

The May 2006 collapse had a higher mass flux than previous dome collapses from the Soufrière Hills volcano. This event deposited coarser grained, thicker deposits further from source than the larger, but more protracted 210 x 10^6 m^3 July 2003 dome collapse; the most voluminous historic lava dome collapse for any volcano. The distal turbidity currents associated with the May 2006 collapse were able to run up 200 m of topography and erode at least 20 cm of underlying volcaniclastic and hemipelagic material at a distance of 24 km from the Montserrat shore. Multiple depositional subunits were emplaced by the May 2006 flows, whereas only single depositional units were emplaced by previous dome collapse pyroclastic flows that were deposited into the ocean (e.g. Trofimovs et al., 2006; 2008). The high volume flux into the ocean together with large flow thickness, relatively high particle loading and the steep slopes on the submarine volcano flanks were likely to have produced the multiple subunits via flow reflection and deflection around seafloor obstacles.

Acknowledgements

This work was supported by the National Environmental Research Council grants NE/D004020/1, NER/A/S/2002/00963 and NE/F010478/1. The authors would like to thank the captain, crew and scientific team on the RRS *James Cook* for their invaluable assistance. Carol Pudsey, Peter Morris and Guy Hannaford are thanked for their technical expertise and advice. B Kneller and V. Manville are thanked for their insightful reviews.

References

Allen JRL (1971) Instantaneous sediment deposition rates deduced from climbing-ripple cross-lamination. Journal of the Geological Society London 127: 553-561

Bonadonna C, Mayberry GC, Calder ES, Sparks RSJ, Choux C, Jackson P, Lejeune A-M, Loughlin SC, Norton GE, Rose WI, Ryan G, Young SR. 2002. Tephra fallout in the eruption of Soufriere Hills Volcano, Montserrat. In: Druitt TH, Kokelaar BP (eds) The Eruption of Soufrière Hills Volcano, Montserrat, from 1995 to 1999. Geol. Soc. London, Memoirs, 21, pp 483-516.

Boudon G, Le Friant A, Komorowski J-C, Deplus C, Semet MP (2007) Volcano flank instability in the Lesser Antilles arc: Diversity of scale, processes, and temporal recurrence. Journal of Geophysical Research – Solid Earth 112 (B8): B08205

Bouma AH (1962) Sedimentology of some Flysch Deposits: A Graphic Approach to Facies Interpretation. Elsevier, Amsterdam

Bouysse P, Westercamp D, Andreieff P (1990) The Lesser Antilles Island Arc. In: Moore JC, Mascle A (eds) Proceedings of the Ocean Drilling Program, scientific results, 110, Ocean Drilling Program, College Station, TX, pp 29–44

Brodscholl A, Kirbani SB, Voight B (2000) Sequential dome-collapse nuees ardentes analyzed from broadband seismic data, Merapi Volcano, Indonesia. Journal of Volcanology and Geothermal Research 100 (1-4): 363-369

Calder ES, Sparks RSJ, Gardeweg MC (2000) Erosion, transport and segregation of pumice and lithic clasts in pyroclastic flows inferred from ignimbrite at Lascar Volcano, Chile. Journal of Volcanology and Geothermal Research 104: 201-235

Carn SA, Watts RB, Thompson G, Norton GE (2004) Anatomy of a lava dome collapse: the 20 March 2000 event at Soufrière Hills Volcano, Montserrat. Journal of Volcanology and Geothermal Research 131 (3-4): 241-264

Cole PD, Calder ES, Sparks RSJ, Clarke AB, Druitt TH, Young SR, Herd RA, Harford CL, Norton GE (2002) Deposits from dome-collapse and fountain-collapse pyroclastic flows at Soufrière Hills Volcano, Montserrat. In: Druitt TH, Kokelaar BP (eds) The Eruption of Soufrière Hills Volcano, Montserrat, from 1995 to 1999. Geol. Soc. London, Memoirs, 21, pp 231-261

Deplus C, Le Friant A, Boudon G, Komorowski J-C, Villemant B, Harford C, Ségoufin J, Cheminée J-L (2001) Submarine evidence for large-scale debris avalanches in the Lesser Antilles Arc. Earth and Planetary Science Letters 192 (2): 145-157

Edmonds M, Herd R (2005) Inland-directed base surge generated by the explosive interaction of pyroclastic flows and seawater at Soufrière Hills volcano, Montserrat. Geology 33: 245-248

Endo ET, Murray TL (1992) Real-time seismic amplitude measurement (RSAM): a volcano monitoring and prediction tool. Bulletin of Volcanology 53: 533-545

Felix G, Thomas N (2004) Relation between dry granular flow regimes and morphology of deposits: formation of levees in pyroclastic deposits. Earth and Planetary Science Letters 221: 197-213

Grindlay NR, Hearne M, Mann P (2005) High risk of tsunami in the Northern Caribbean. EOS Transactions, American Geophysical Union 86 (12): 121-132

Harford CL, Pringle MS, Sparks RSJ, Young SR (2002) The volcanic evolution of Montserrat using $^{40}Ar/^{39}Ar$ geochronology. In: Druitt TH, Kokelaar BP (eds) The eruption of Soufrière Hills volcano, Montserrat, from 1995 to 1999. Geological Society of London, Memoir 21 pp 93-113

Hart K, Carey S, Sigurdsson H, Sparks RSJ, Robertson REA (2004) Discharge of pyroclastic flows into the sea during the 1996-1998 eruptions of the Soufrière Hills volcano, Montserrat. Bulletin of Volcanology 66: 599-614

Herd RA, Edmonds M, Bass V (2006) Catastrophic lava dome failure at Soufrière Hills Volcano, Montserrat 12-13 July 2003. Journal of Volcanology and Geothermal Research 148 (3-4): 234-252

Jones LD (2006) Monitoring landslides in hazardous terrain using LiDAR: an example from Montserrat. Quarterly Journal of Engineering Geology and Hydrogeology 39: 371-373

Kneller BC, Buckee C (2000) The structure and fluid mechanics of turbidity currents: a review of some recent studies and their geological implications. Sedimentology 47: 62-94

Kneller BC, McCaffrey WD (1999) Depositional effects of flow non-uniformity and stratification within turbidity currents approaching a bounding slope: deflection, reflection and facies variation. Journal of Sedimentary Research 69: 980-991

Kneller BC, McCaffrey WD (2003) The interpretation of vertical sequences in turbidite beds: The influence of longitudinal flow structure. Journal of Sedimentary Research 73 (5): 706-713

Kokelaar BP (2002) Setting, chronology and consequences of the eruption of Soufrière Hills volcano, Montserrat (1995-1999). In: Druitt TH, Kokelaar BP (eds) The eruption of Soufrière Hills volcano, Montserrat, from 1995 to 1999. Geological Society of London, Memoir, 21 pp 1-44.

Kuenen PH (1966) Matrix of turbidites: experimental approach. Sedimentology 7: 267-297

Le Friant A, Harford CL, Deplus C, Boudon G, Sparks RSJ, Herd RA, Komorowski J-C (2004) Geomorphological evolution of Montserrat (West Indies): importance of flank collapse and erosional processes. Journal of the Geological Society London 161: 147-160

Le Friant A, Deplus C, Boudon G, Sparks RSJ, Trofimovs J, Talling PJ (2009) Submarine deposition of volcaniclastic material from the 1995-2005 eruptions of Soufrière Hills volcano, Montserrat. Journal of the Geological Society, London 166: 171-182

Loughlin SC et al. (2006). Report to the Scientific Advisory Committee, Montserrat, August 2006 (06/07), open file report, Montserrat Volcano Observatory, Flemmings, Montserrat

Loughlin SC, Luckett R, Ryan G, Christopher T, Hards V, De Angelis S, Jones L, Strutt M (2010) An overview of lava dome evolution, dome collapse and cyclicity at

Soufriere Hills Volcano, Montserrat, 2005-2007. Geophysical Research Letters, 37, L00E16, doi:10.1029/2010GL042547

Loughlin SC, Baxter PJ, Aspinall WP, Darroux B, Harford CL, Miller AD (2002) Eyewitness accounts of the 25 June 1997 pyroclastic flows at Soufrière Hills Volcano, Montserrat, and implications for disaster mitigation. In: 'The eruption of Soufrière Hills Volcano, Montserrat, from 1995 to 1999'. In: Druitt TH, Kokelaar BP (eds) The Eruption of Soufrière Hills Volcano, Montserrat, from 1995 to 1999. Geol. Soc. London, Memoirs, 21, pp 211-230

Lube G, Cronin SJ, Platz T, Freundt A, Procter JN, Henderson C, Sheridan MF (2007) Flow and deposition of pyroclastic granular flows: A type example from the 1975 Ngauruhoe eruption, New Zealand. Journal of Volcanology and Geothermal Research 161: 165-186

Luckett R, Loughlin S, De Angelis S, Ryan G (2008) Volcanic seismicity at Montserrat, a comparison between the 2005 dome growth episode and earlier dome growth. Journal of Volcanology and Geothermal Research, 177 (4), 894-902, doi: 10.1016/j.jvolgeores.2008.07.006

Nairn IA, Self S (1978) Explosive eruptions and pyroclastic avalanches from Ngauruhoe in February 1975. Journal of Volcanology and Geothermal Research 3: 39-60

Rodriguez-Elizarraras S, Siebe S, Komorowski J-C, Expindola J-M, Saucedo R (1991) Field observations of pristine block and ash flow deposits emplaced April 16-17, 1991 at Volcan de Colima, Mexico. Journal of Volcanology and Geothermal Research 48: 399-412

Roobol MJ, Smith AL (1998) Pyroclastic stratigraphy of the Soufrière Hills volcano, Montserrat: Implications for the present eruption. Geophysical Research Letters 25: 3393-3396

Ryan GA, Loughlin SC, James MR, Jones LD, Calder ES, Christopher T, Strutt MH, Wadge G (2010) Growth of the lava dome and extrusion rates at Soufrière Hills Volcano, Montserrat, West Indies: 2005-2008. Geophysical Research Letters 37: L00E08, doi:10.1029/2009GL041477

Saucedo R, Macais JL, Bursik M (2004) Pyroclastic flows deposits of the 1991 eruption of Volcan de Colima, Mexico. Bulletin of Volcanology 66: 291-306

Trofimovs J, Amy L, Boudon G, Deplus C, Doyle E, Fournier N, Hart MB, Komorowski J-C, Le Friant A, Lock EJ, Pudsey C, Ryan G, Sparks RSJ, Talling PJ (2006) Submarine pyroclastic deposits formed at the Soufrière Hills Volcano, Montserrat (1995-2003): what happens when pyroclastic flows enter the ocean? Geology 34 (7): 549-552

Trofimovs J, Sparks RSJ, Talling PJ (2008) Anatomy of a submarine pyroclastic flow and associated turbidity current: July 2003 dome collapse, Soufrière Hills volcano, Montserrat, West Indies. Sedimentology 55: 617-634

Ui T, Matsuwo N, Sumita M, Fujinawa A (1999) Generation of block and ash flows during the 1990-1995 eruption of Unzen Volcano, Japan. Journal of Volcanology and Geothermal Research 89 (1-4): 123-137

Voight B, Linde AT, Sacks IS, Mattioli GS, Sparks RSJ, Elsworth D, Hidayat D, Malin PE, Shalev E, Widiwijayanti C, Young SR, Bass V, Clarke A, Dunkley P, Johnston W, McWhorter N, Neuberg J, Williams P (2006) Unprecedented pressure increase in deep magma reservoir triggered by lava-dome collapse. Geophysical Research Letters 33 (3): L03312

Figure captions

Fig. 1. Map showing the location of Montserrat within the Lesser Antilles Island Arc (inset), seafloor topography and core locations. Bathymetric contours are shown in metres. SP denotes Spanish Point.

Fig. 2. Photograph taken on the 21st of May 2006 showing the pyroclastic fan at the base of the Tar River Valley. Note the erosive channel (bound by dashed lines) in the centre of the fan marking the axis of the pyroclastic flow. Photo courtesy of NERC/Government of Montserrat.

Fig. 3. A) Bathymetric survey offshore from the base of the Tar River Valley from the JR123 cruise in May 2005. B) Bathymetric survey offshore from the base of the Tar River Valley from the JC18 cruise in December 2007. R shows the linear ridge at 16.72° N. D marks a linear depression in the proximal part of the ridge in the JC18

bathymetric survey. The red dashed line marks the submarine extension of the southern scarp of the subaerial Tar River Valley (termed C1 in Le Friant et al., 2004).

Fig. 4. A) Topographic difference map showing the difference in seafloor depths between the 2005 JR123 bathymetric survey and the December 2007 JC18 bathymetric survey. TRV = Tar River Valley. Pre-May 2006 dome collapse bathymetry is shown with 100 m contours. B) Topographic difference map between the 2005 and 2007 bathymetric surveys draped over a 3D visualization of the December 2007 seafloor bathymetry. This image has a vertical exaggeration of 3. The colour scale corresponds to: green to red = 0-50 m deposition, blue and magenta = 0-40 m erosion.

Fig. 5. Longitudinal seafloor profile along the axis of the May 2006 proximal pyroclastic ridge. Vertical exaggeration = ×8. The red line shows the pre-eruption seafloor from the 1985 HMS Fawn survey, the green line shows the 2005 JR123 cruise survey and the blue line shows the 2007 JC18 survey.

Fig. 6. A) JC18 bathymetry map showing the location of the seafloor profiles shown in Figures 6B, 6C and 6D. B) South to north seafloor profile X-X′ along longitude 62.1272° W. The HMS Fawn profile (red) has been generated from fewer data points than the JR123 2005 profile (green) or the 2007 JC18 profile (blue). Therefore the red profile appears more staggered than the younger surveys. The areas of extreme deposition and erosion are likely to be artifacts of the paucity of the pre-eruption data. C) South to north seafloor profile Y-Y′ along longitude 62.1085° W. Coloured lines and data are as described for 6B. D) South to north seafloor profile Z-Z′ along longitude 62.0956° W. Coloured lines and data are as described for 6B.

Fig. 7. Isopach map showing the thickness distribution of the submarine deposits of the May 2006 dome collapse. Isopach contours are as marked in centimetres. Individual core thickness measurements are given in centimetres. The imaged proximal deposits greater than or equal to 10 m are shown offshore from the base of the Tar River Valley.

Fig. 8. Correlative stratigraphic logs showing the May 2006 dome collapse deposits north to south along the axis of the Bouillante-Montserrat graben. Inset map traces the logged profile down the graben.

Fig. 9. Correlative stratigraphic logs for an east west transect perpendicular to the main flow axis. The number of depositional units increases towards the graben margins. Inset map shows the location of the transect.

Fig. 10. Detailed grain size analysis of megacore JC18-7-M (16° 41.00' N, 62° 02.00'W).

Fig. 11. Detailed grain size analysis of boxcore JC18-10-B (16°33.00' N, 62° 00.00' W). The stratigraphic log of core JR123-8-V (16° 33.51' N, 61° 59.49' W), recovered in May 2005, is shown for comparison.

Fig. 12. Detailed grain size analysis of megacore JC18-12-M (16° 24.80' N, 61° 54.50' W).

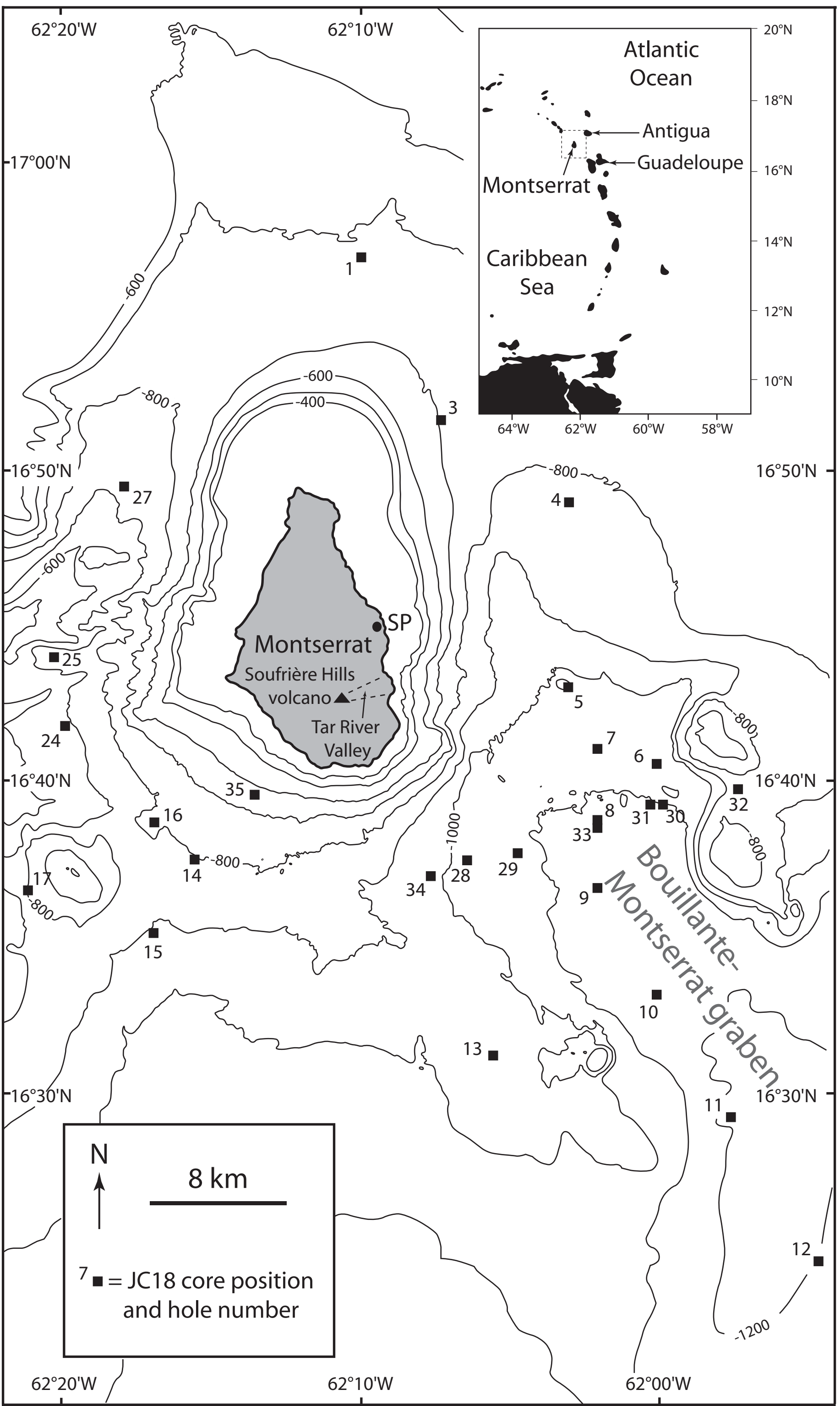

62°20'W
62°10'W
17°00'N
16°50'N
16°40'N
16°30'N
62°00'W
-600
-800
-400
-1000
-1200
Montserrat
SP
Soufrière Hills volcano
Tar River Valley
Bouillante-Montserrat graben
1
3
4
5
6
7
8
9
10
11
12
13
14
15
16
17
24
25
27
28
29
30
31
32
33
34
35
Atlantic Ocean
Antigua
Guadeloupe
Montserrat
Caribbean Sea
20°N
18°N
16°N
14°N
12°N
10°N
64°W
62°W
60°W
58°W
N
8 km
7 = JC18 core position and hole number


N
channel

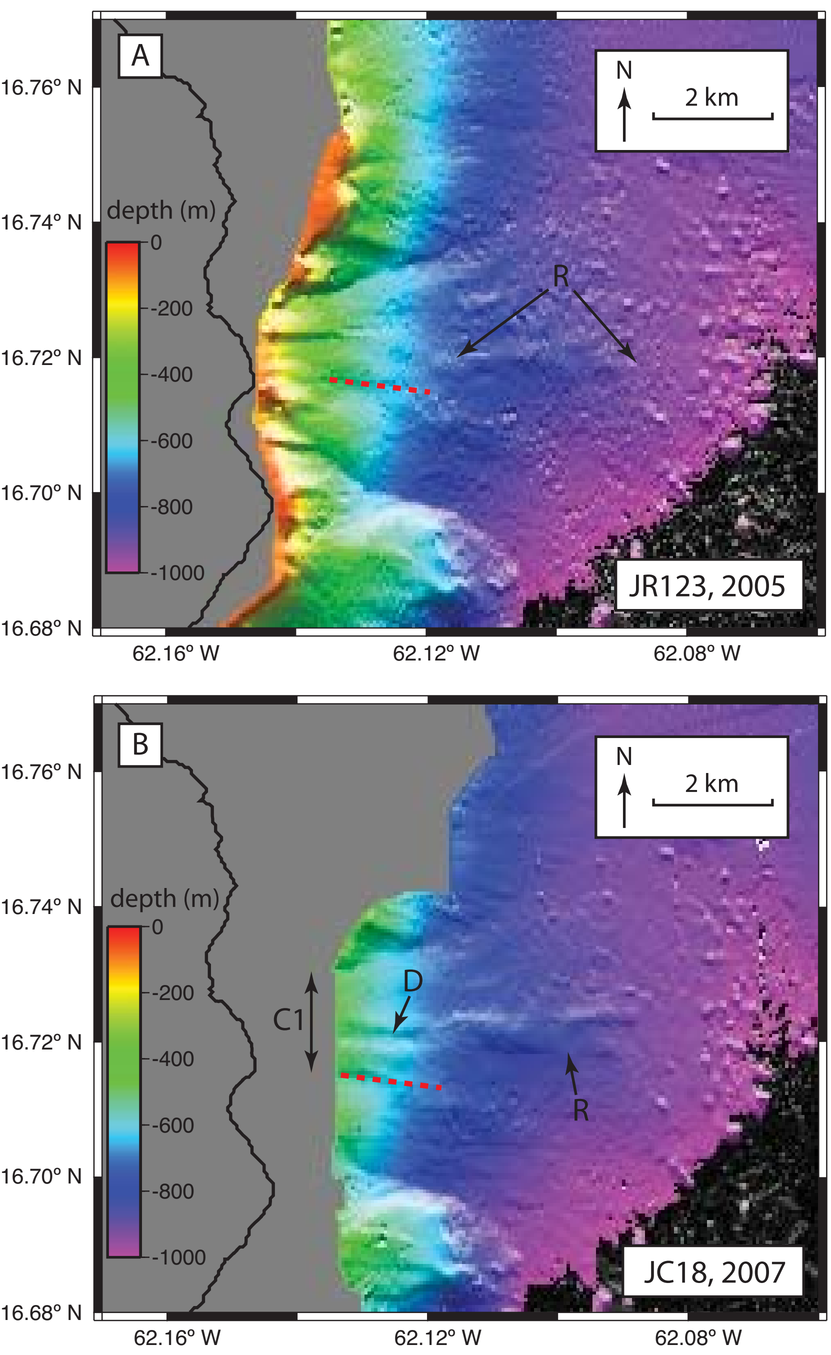
A
N
2 km
depth (m)
0
-200
-400
-600
-800
-1000
R
JR123, 2005
16.76° N
16.74° N
16.72° N
16.70° N
16.68° N
62.16° W
62.12° W
62.08° W
B
N
2 km
depth (m)
0
-200
-400
-600
-800
-1000
C1
D
R
JC18, 2007
16.76° N
16.74° N
16.72° N
16.70° N
16.68° N
62.16° W
62.12° W
62.08° W

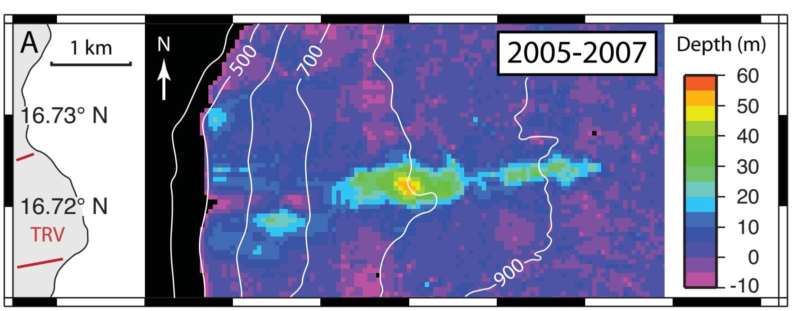
A
1 km
N
16.73° N
16.72° N
TRV
500
700
900
2005-2007
Depth (m)
60
50
40
30
20
10
0
-10
62.14° W
62.12° W
62.10° W
62.08° W

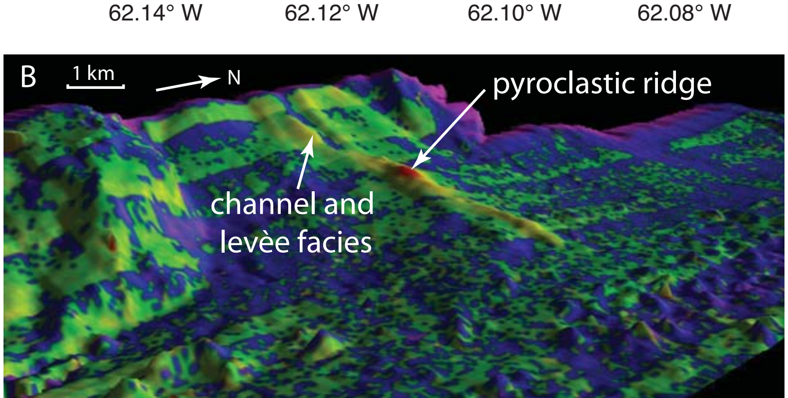
B
1 km
N
pyroclastic ridge
channel and
levèe facies

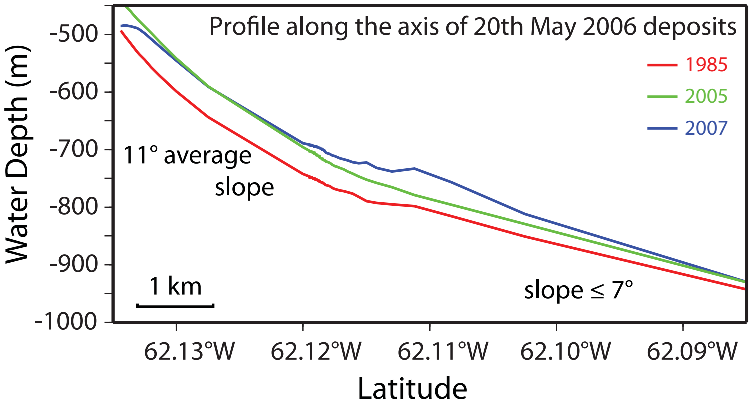

Profile along the axis of 20th May 2006 deposits
1985
2005
2007
Water Depth (m)
-500
-600
-700
-800
-900
-1000
11° average slope
slope ≤ 7°
1 km
62.13°W
62.12°W
62.11°W
62.10°W
62.09°W
Latitude

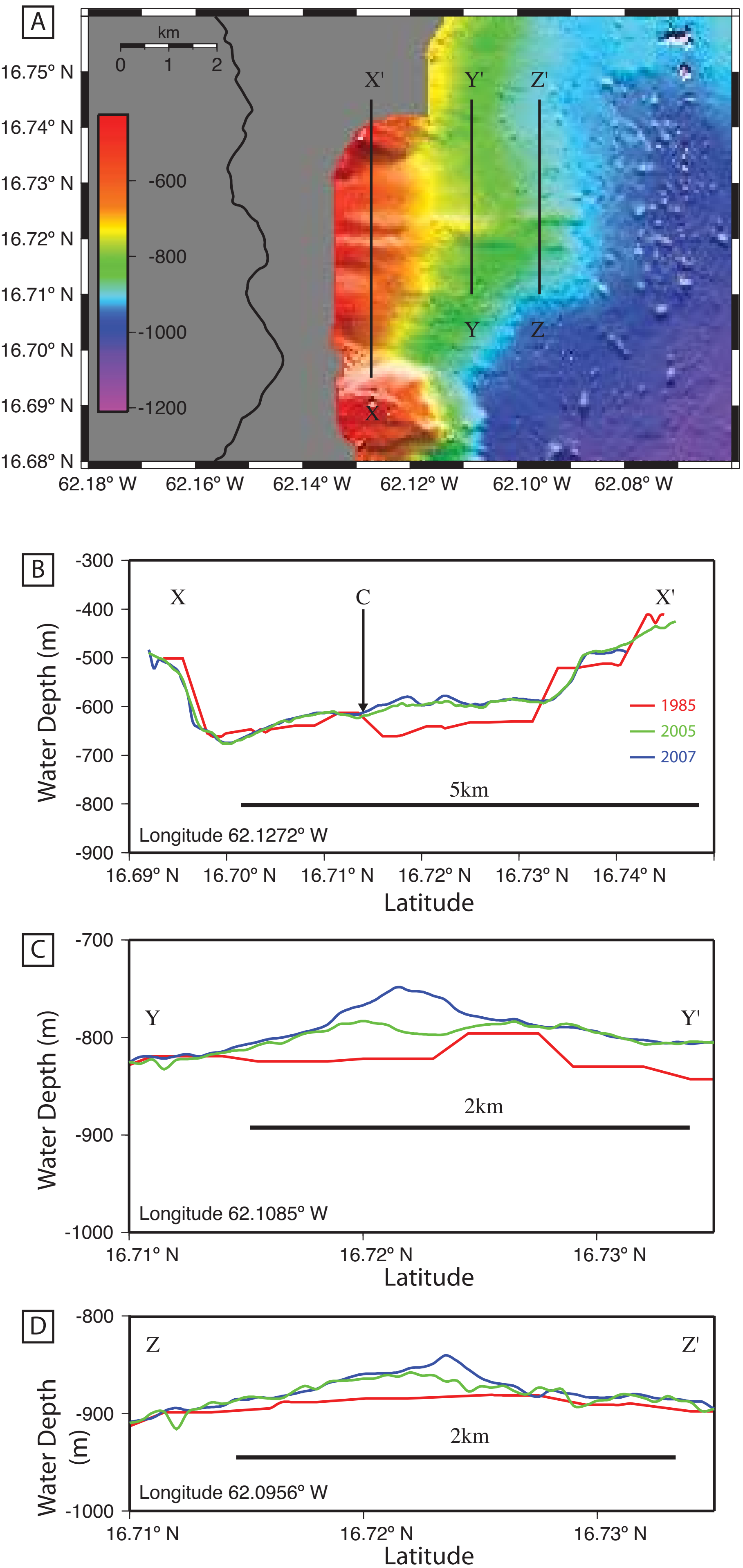

A
km
0 1 2
-600
-800
-1000
-1200
X' Y' Z'
X Y Z
16.75° N
16.74° N
16.73° N
16.72° N
16.71° N
16.70° N
16.69° N
16.68° N
62.18° W 62.16° W 62.14° W 62.12° W 62.10° W 62.08° W
B
Water Depth (m)
X C X'
1985
2005
2007
5km
Longitude 62.1272° W
16.69° N 16.70° N 16.71° N 16.72° N 16.73° N 16.74° N
Latitude
C
Y Y'
2km
Longitude 62.1085° W
16.71° N 16.72° N 16.73° N
Latitude
D
Z Z'
2km
Longitude 62.0956° W
Water Depth (m)
16.71° N 16.72° N 16.73° N
Latitude

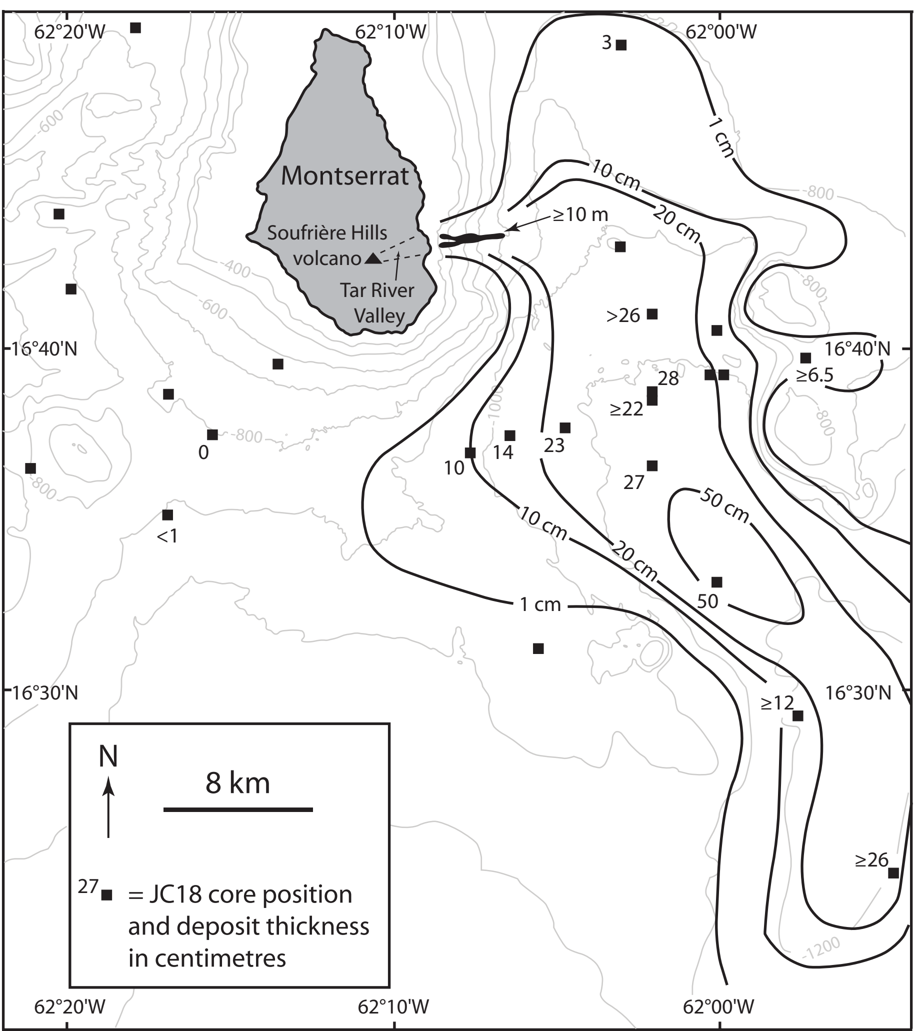

62°20'W
62°10'W
62°00'W
Montserrat
Soufrière Hills
volcano
Tar River
Valley
≥10 m
1 cm
10 cm
20 cm
50 cm
3
>26
28
≥22
≥6.5
10
14
23
27
50
0
<1
≥12
≥26
16°40'N
16°30'N
-400
-600
-800
-1200
N
8 km
27 = JC18 core position and deposit thickness in centimetres

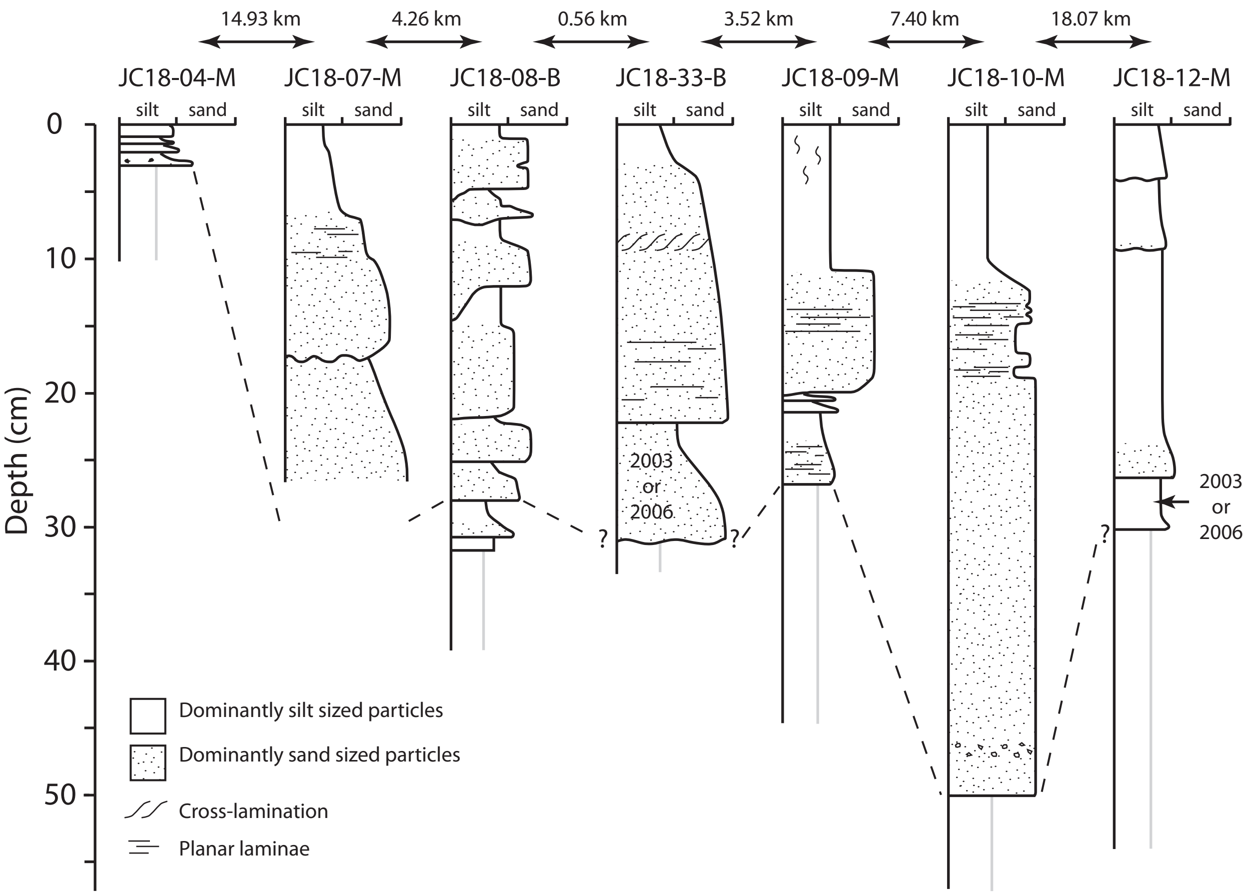
14.93 km
4.26 km
0.56 km
3.52 km
7.40 km
18.07 km
JC18-04-M
JC18-07-M
JC18-08-B
JC18-33-B
JC18-09-M
JC18-10-M
JC18-12-M
silt
sand
Depth (cm)
0
10
20
30
40
50
2003 or 2006
2003 or 2006
?
Dominantly silt sized particles
Dominantly sand sized particles
Cross-lamination
Planar laminae

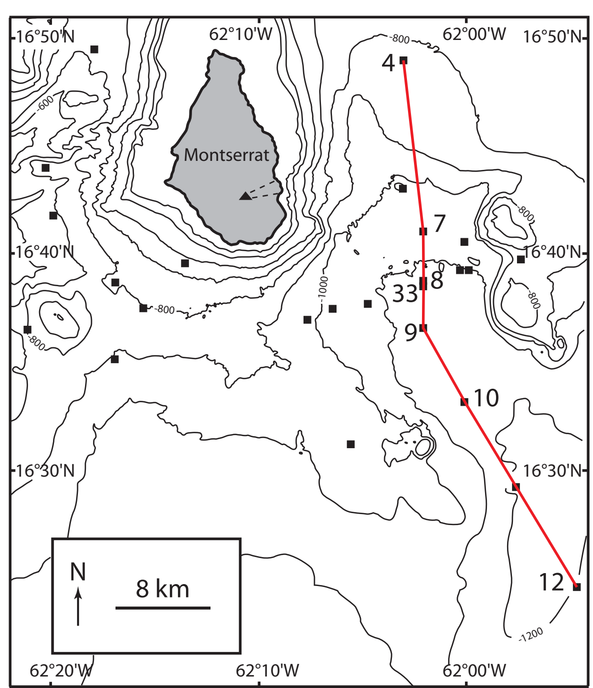
16°50'N
62°10'W
62°00'W
16°40'N
16°30'N
62°20'W
Montserrat
4
7
8
33
9
10
12
-800
-600
-1000
-1200
N
8 km

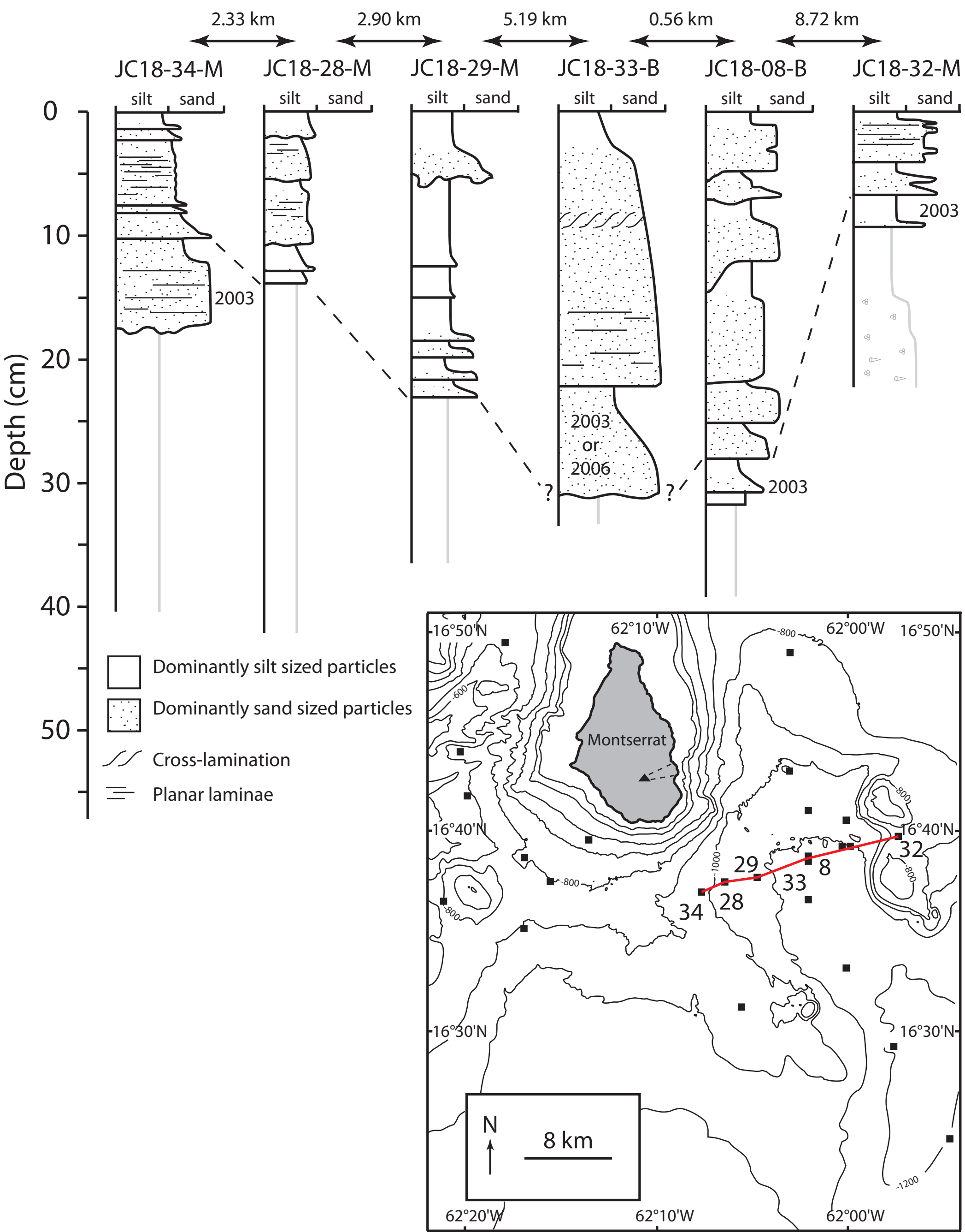

2.33 km
2.90 km
5.19 km
0.56 km
8.72 km
JC18-34-M
JC18-28-M
JC18-29-M
JC18-33-B
JC18-08-B
JC18-32-M
silt
sand
Depth (cm)
0
10
20
30
40
50
2003
2003
or
2006
?
Dominantly silt sized particles
Dominantly sand sized particles
Cross-lamination
Planar laminae
16°50'N
62°10'W
62°00'W
16°40'N
16°30'N
62°20'W
Montserrat
-800
-600
-1000
-1200
29
8
33
32
34
28
N
8 km

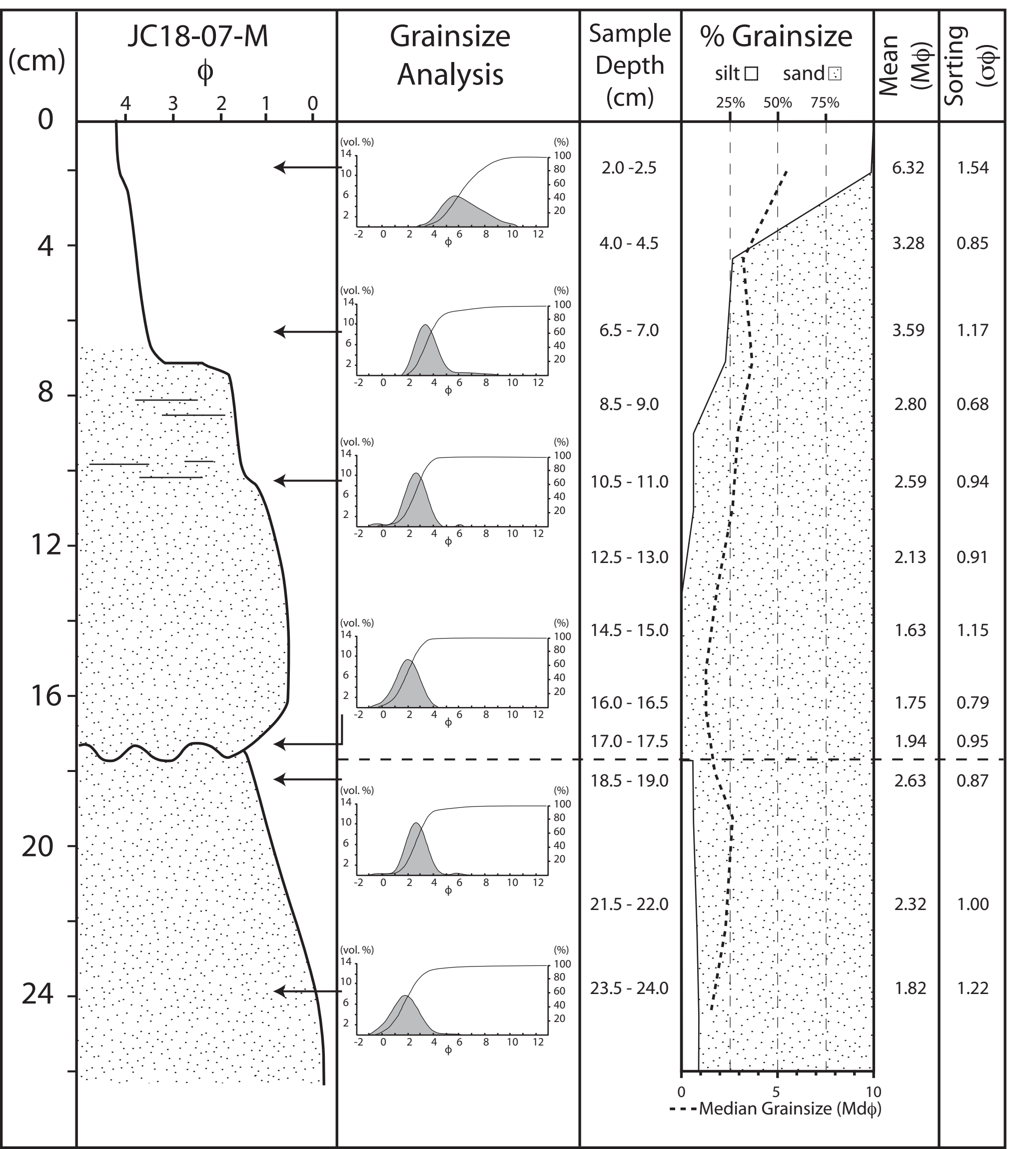

(cm)
JC18-07-M
ϕ
4 3 2 1 0
Grainsize Analysis
Sample Depth (cm)
% Grainsize
silt
sand
25% 50% 75%
Mean (Mϕ)
Sorting (σϕ)
0
4
8
12
16
20
24
(vol. %)
(%)
2.0 -2.5
4.0 - 4.5
6.5 - 7.0
8.5 - 9.0
10.5 - 11.0
12.5 - 13.0
14.5 - 15.0
16.0 - 16.5
17.0 - 17.5
18.5 - 19.0
21.5 - 22.0
23.5 - 24.0
6.32 1.54
3.28 0.85
3.59 1.17
2.80 0.68
2.59 0.94
2.13 0.91
1.63 1.15
1.75 0.79
1.94 0.95
2.63 0.87
2.32 1.00
1.82 1.22
0 5 10
Median Grainsize (Mdϕ)

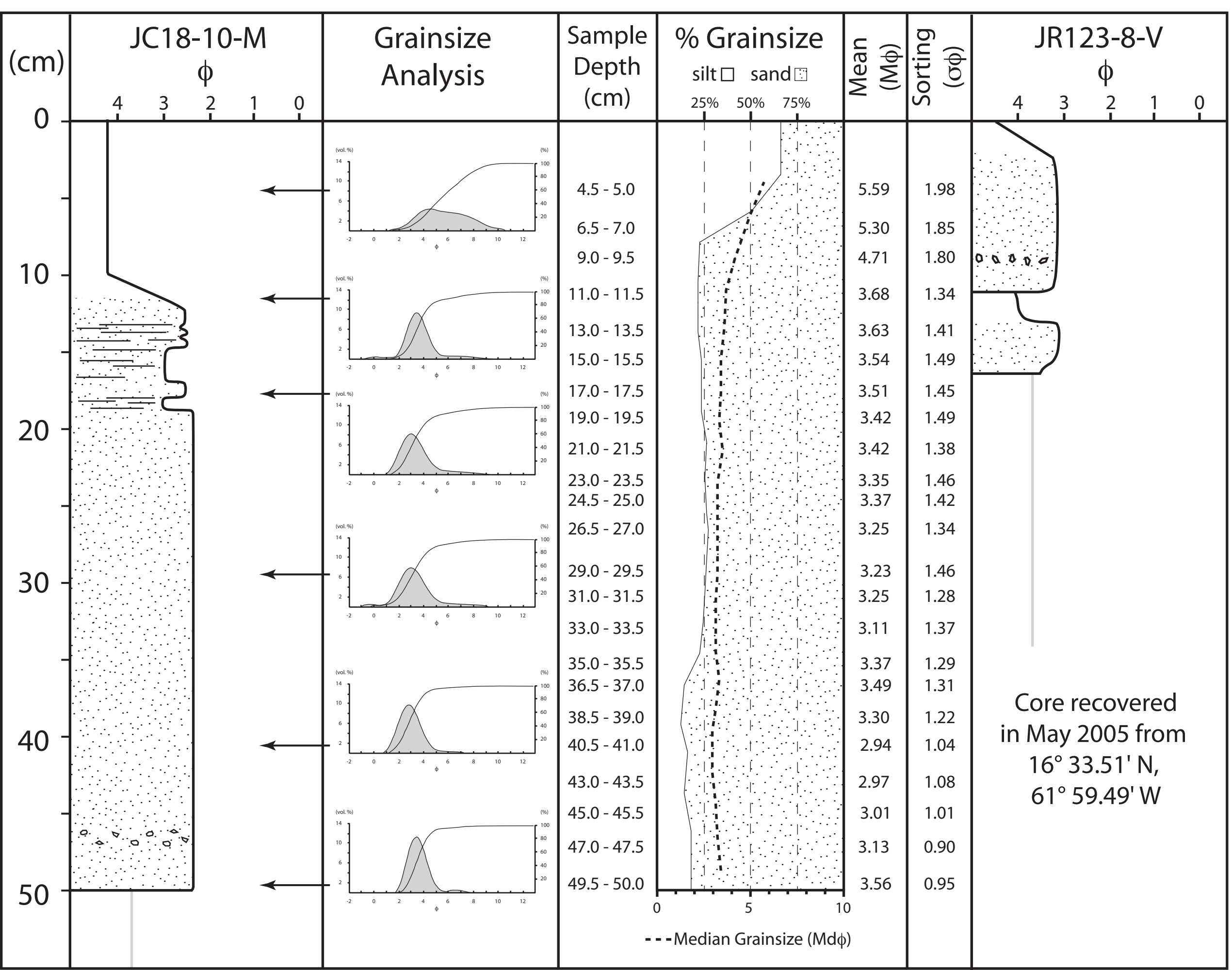
(cm)
JC18-10-M
φ
Grainsize Analysis
Sample Depth (cm)
% Grainsize
silt
sand
25%
50%
75%
Mean (Mφ)
Sorting (σφ)
JR123-8-V
φ
4.5 - 5.0 5.59 1.98
6.5 - 7.0 5.30 1.85
9.0 - 9.5 4.71 1.80
11.0 - 11.5 3.68 1.34
13.0 - 13.5 3.63 1.41
15.0 - 15.5 3.54 1.49
17.0 - 17.5 3.51 1.45
19.0 - 19.5 3.42 1.49
21.0 - 21.5 3.42 1.38
23.0 - 23.5 3.35 1.46
24.5 - 25.0 3.37 1.42
26.5 - 27.0 3.25 1.34
29.0 - 29.5 3.23 1.46
31.0 - 31.5 3.25 1.28
33.0 - 33.5 3.11 1.37
35.0 - 35.5 3.37 1.29
36.5 - 37.0 3.49 1.31
38.5 - 39.0 3.30 1.22
40.5 - 41.0 2.94 1.04
43.0 - 43.5 2.97 1.08
45.0 - 45.5 3.01 1.01
47.0 - 47.5 3.13 0.90
49.5 - 50.0 3.56 0.95
Median Grainsize (Mdφ)
Core recovered in May 2005 from 16° 33.51' N, 61° 59.49' W

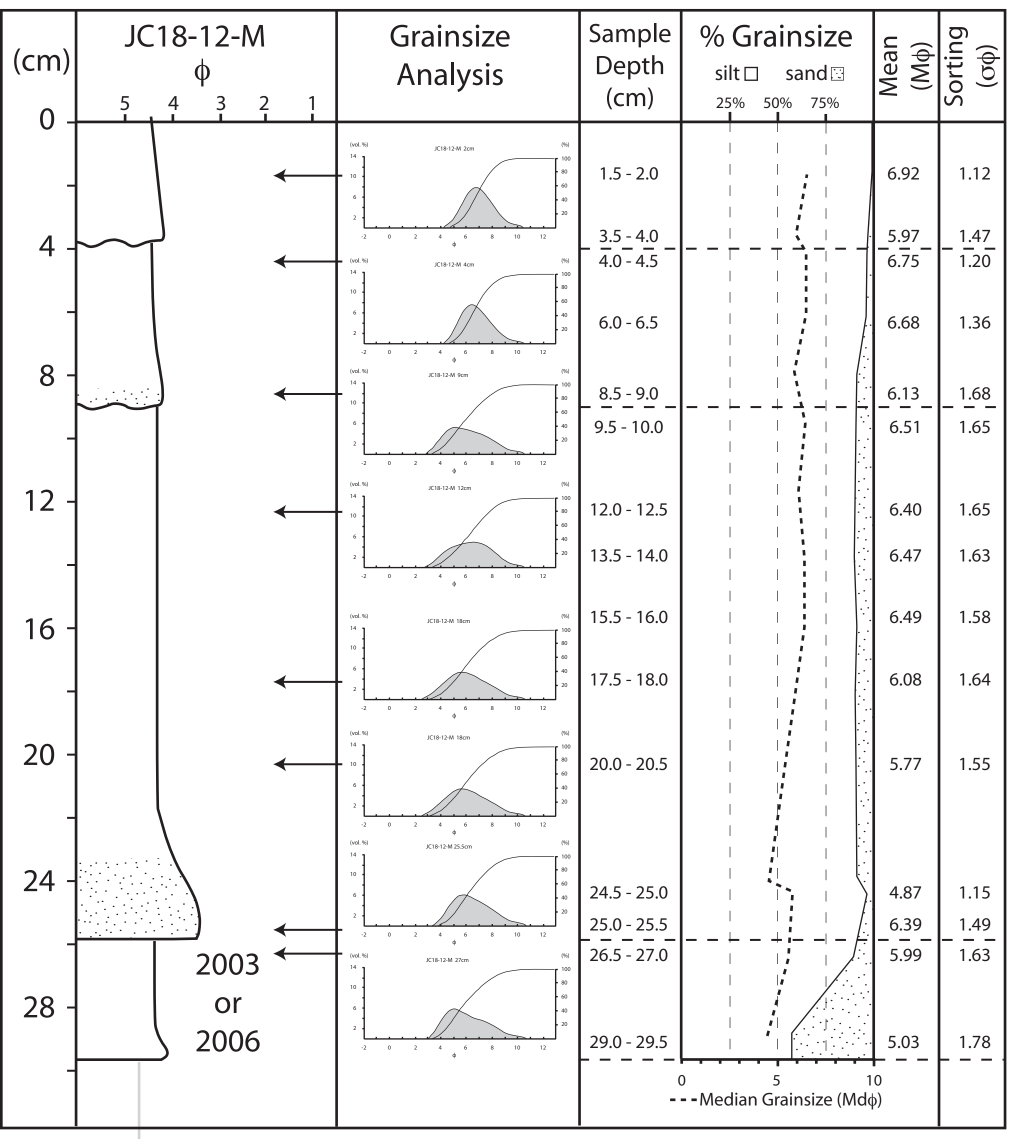

(cm)
JC18-12-M
ϕ
5 4 3 2 1
Grainsize Analysis
Sample Depth (cm)
% Grainsize
silt
sand
25%
50%
75%
Mean (Mϕ)
Sorting (σϕ)
0
4
8
12
16
20
24
28
2003 or 2006
1.5 - 2.0
3.5 - 4.0
4.0 - 4.5
6.0 - 6.5
8.5 - 9.0
9.5 - 10.0
12.0 - 12.5
13.5 - 14.0
15.5 - 16.0
17.5 - 18.0
20.0 - 20.5
24.5 - 25.0
25.0 - 25.5
26.5 - 27.0
29.0 - 29.5
6.92
5.97
6.75
6.68
6.13
6.51
6.40
6.47
6.49
6.08
5.77
4.87
6.39
5.99
5.03
1.12
1.47
1.20
1.36
1.68
1.65
1.65
1.63
1.58
1.64
1.55
1.15
1.49
1.63
1.78
0
5
10
Median Grainsize (Mdϕ)